Local Lattice Effects in the Layered Manganite $La_{1.4}Sr_{1.6}Mn_2O_7$

Despina Louca and G. H. Kwei
Los Alamos National Laboratory, Los Alamos, New Mexico 87545

J. F. Mitchell
Argonne National Laboratory, Argonne, Illinois 60439

(Received 18 November 1997)

The pair density function analysis of pulsed neutron diffraction data for the two-layer manganite $La_{1.4}Sr_{1.6}Mn_2O_7$ indicates the presence of a large local Jahn-Teller (JT) distortion of comparable magnitude to that found in the perovskites, while the crystallographic structure shows a very small JT effect. A model that includes JT displacements provides a better representation of the local structure than the existing crystallographic one. While the local distortion is reduced at lower temperatures its change corresponds more to the increase in the transport in the *ab* plane than to the magnetic transition, reflecting the 2D nature of the crystal. [S0031-9007(98)05871-2]

PACS numbers: 71.38.+i, 61.12.–q, 71.30.+h, 75.70.Pa

The phenomenon of colossal magnetoresistance (CMR) renewed the interest in manganites with the general composition of $(La/Sr)_{n+1}Mn_nO_{3n+1}$ [1]. The correlation between magnetism and transport that gives rise to the CMR effect is still under investigation. While the double exchange (DE) interaction coupling the charge to the spin degrees of freedom in the ferromagnetic (FM) metallic state was originally proposed for the $n = \infty$ member ($La_{1-x}A_xMnO_3$) [2], experimental evidence suggested a mechanism [3] requiring a lattice contribution [4]. A number of studies showed significant structural changes coinciding with the transition in the properties [5,6] in accordance with the presence of lattice polarons. Similar properties have recently been observed in the layered compounds but with no clear evidence for polarons or a full Jahn-Teller (JT) distortion in this system.

In the $n = 2$ series, the observed magnetoresistance effect is even stronger than in the perovskites but occurs at a lower Curie temperature T_C [7]. The average structure is tetragonal, made of a bilayer perovskite unit in the *ab* plane of the crystal, separated by a single rocksalt-type La/Sr-O layer along the *c* axis giving it a 2D character [8]. The separation of the octahedra inhibits both the interlayer magnetic coupling and the electrical conductivity. The coupling in the *ab* plane is greater by 1 order of magnitude than along the *c* axis. This can be simply understood from the presence of the nonmagnetic (La/Sr)-O layer. Similarly, the transport measurements in single crystals show that the resistivity along the *c* axis is about 2 orders of magnitude greater than across the *ab* plane [7]. The resistivity profile in the *ab* plane is quite different from the *c* axis as it shows a transition at a considerably higher temperature [9], close to the one observed in the perovskite system at comparable doping.

A recent magnetic neutron scattering measurement on a $La_{2-2x}Sr_{1+2x}Mn_2O_7$ sample with $x = 0.4$ provided evidence for the existence of short range antiferromagnetic (AFM) correlations in the paramagnetic (PM) state [10]. It was suggested that the presence of such domains might induce deviations from the average crystallographic structure. Indeed, our pulsed neutron powder diffraction study on $La_{1.4}Sr_{1.6}Mn_2O_7$ ($x = 0.3$) indicates that, similarly to the perovskites, the lattice is actively involved in the properties of this system. It is the objective of this paper to show that local lattice distortions stem from a JT effect. The local distortions may be connected with the domains of AFM correlations. This study provides the first clear observation of a full JT distortion in this system while an earlier study [11] suggested a very small average JT effect (a change of 0.024 Å in the MnO atomic displacements) in an $x = 0.4$ sample, which is minute in comparison to the local changes observed here (0.2 Å).

The sample was prepared by standard ceramic methods and fired several times at high temperature to achieve a single phase. No significant (less than 1%–2%) secondary phases were identified from the Rietveld refinement of the structure from the diffraction data. The sample was characterized by resistivity and magnetization measurements and the FM transition occurs at 116 K which coincides with the insulator-metal (IM) transition (Fig. 1). The neutron diffraction data were collected using the special environment powder diffractometer (SEPD) of the intense pulsed neutron source (IPNS) of the Argonne National Laboratory. Data were collected from room temperature (RT) to 20 K. Data at a finer temperature spaced grid were collected at a later time. The structure function $S(Q)$, determined up to 33 $Å^{-1}$, was Fourier transformed to obtain the pair density function (PDF) $\rho(r)$. The PDF analysis provides direct information with regard to the local structure without a requirement of long range structural periodicity. Its application extends beyond the amorphous materials to crystalline solids as well [12].

The local octahedral environment is particularly sensitive to the charge distribution providing direct evidence for the response of the lattice to the change in the

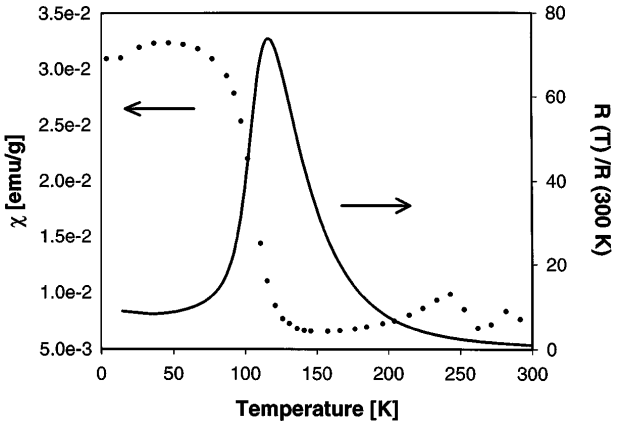

FIG. 1. A plot of the resistance and susceptibility as a function of temperature. The transition occurs at 116 K. Single crystal measurements [9] showed that ρ_c is 3000 times larger than ρ_{ab} and that the T_C of ρ_{ab} is higher than the T_C of ρ_c where the latter coincides with the FM transition.

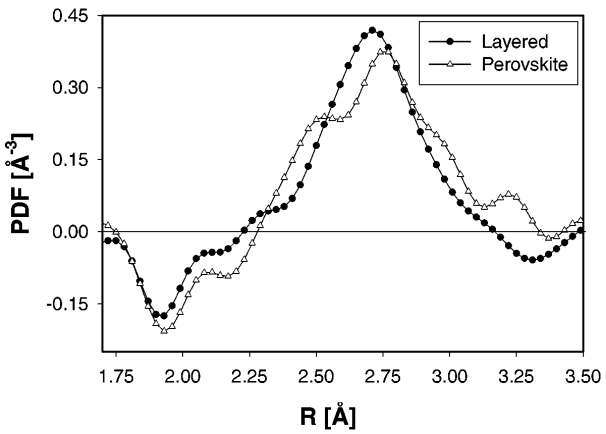

FIG. 2. The local structure of the layered compound is compared to the one obtained from the pure $LaMnO_3$ at RT. Note that a split in the Mn-O peak is seen, at 1.92 and at 2.12 Å, corresponding to short and long bonds in the layered material, respectively, and is as pronounced as the one observed in the perovskite. This serves as a strong indication that the Jahn-Teller distortion is present in this system as in the perovskites.

transport. In $La_{1.4}Sr_{1.6}Mn_2O_7$, the nominal valence is $Mn^{3.3+}$ but the actual electronic charge on Mn can vary from 3+ to 4+. If carriers are localized and the system is made of Mn^{3+} and Mn^{4+} ions, it is possible to structurally identify the Mn^{4+} ions in a matrix of Mn^{3+}, and vice versa, from the distinct environment associated with the Mn^{3+} and Mn^{4+} octahedra. A Mn^{3+} octahedron is elongated because of the JT effect induced by the presence of an electron in the e_g orbital. Of the six Mn-O bonds around manganese, some of them will be longer than average because of the filling of the antibonding $Mn(3d_{z^2})$-$O(2p)$ σ^* band. This is clearly the case in the pure perovskite (with Mn^{3+} ions only) where a distribution of four short and two long bonds is observed [6,13]. On the other hand, the octahedron associated with the Mn^{4+} is undistorted because it is JT-free and all Mn-O bonds are of the same average length as in $CaMnO_3$ [14]. If the charge carriers are fully delocalized, however, the holes will be uniformly distributed over all sites and all Mn-O bonds will be of about the same length.

In Fig. 2 the PDF of the layered manganite $La_{1.4}Sr_{1.6}Mn_2O_7$ determined at RT is compared to that of pure $LaMnO_3$ [6]. The first two negative peaks at 1.92 and 2.12 Å correspond to two types of Mn-O bond lengths within the octahedron and they are negative because the neutron scattering length of manganese is negative. It is quite surprising to observe that the Mn-O distances are split in the layered material similarly to the pure perovskite with the long Mn-O bond at 2.18 Å [6]. This is not expected from the average crystallographic structure since it gives only the range of Mn-O bonds from 1.93–2.03 Å and the octahedra in the bilayer are almost perfect. As seen from the local structure though, the magnitude of the distortion in the layered system is as significant as in $LaMnO_3$ suggesting that Mn^{3+} ions exist in the PM state providing the long MnO bonds. This implies that a JT distortion is present in the layered manganites where it is sometimes referred to as a pseudo-JT effect in the absence of cubic symmetry of the layered material but with similar consequences [15]. Hence at RT some holes are localized giving rise to a mixed charge state for Mn.

In addition, in Fig. 3 we compare the PDF of the layered compound at RT (symbols) to a model PDF calculated from the crystallographic structure with the

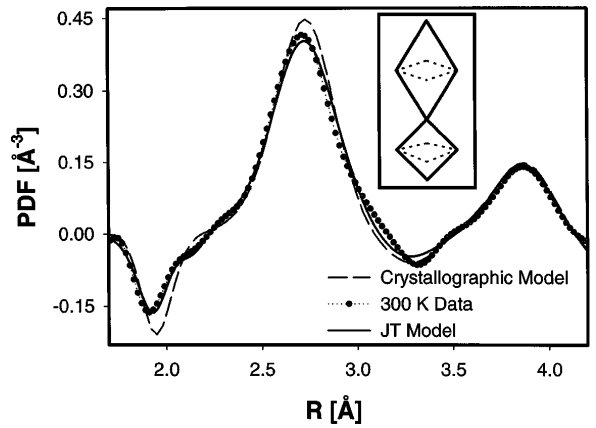

FIG. 3. The PDF of $La_{1.4}Sr_{1.6}Mn_2O_7$ at RT (symbols) is compared to the crystallographic model PDF (dashed line). The model PDF is constructed of δ functions corresponding to interatomic distances in the structure. The sum of the partial PDF's for each atom gives the total PDF of the crystal convoluted with a Gaussian function to simulate thermal and quantum zero point vibrations [12]. Note that the split of the Mn-O peak seen in the data PDF is not present in the model PDF which represents the average crystal structure. However, the new JT model PDF (solid line) which includes JT distortions at 50% of the Mn sites as proposed from modeling the local structure (inset) provides a better agreement to the data.

TABLE I. Mean amplitude of oscillations, $\langle u_{ii}^2 \rangle^{1/2}$ (Å), determined from the thermal factor $B = 8\pi^2 \langle u_{ii}^2 \rangle$ at RT and 20 K for the three types of oxygen atoms. (RS = rocksalt; OH = octahedron).

	$\langle u_{11}^2 \rangle^{1/2}$		$\langle u_{22}^2 \rangle^{1/2}$		$\langle u_{33}^2 \rangle^{1/2}$	
	20 K	RT	20 K	RT	20 K	RT
O1 (Axial, OH)	0.102	0.127	$\langle u_{11}^2 \rangle^{1/2}$		0.079	0.095
O2 (Planar)	0.067	0.095	0.064	0.085	0.118	0.136
O3 (Axial, RS)	0.112	0.130	$\langle u_{11}^2 \rangle^{1/2}$		0.122	0.148

$I/4mmm$ symmetry (dashed line). The parameters for the model are obtained from the Rietveld refinement of the same data used for the PDF analysis. As seen, the experimental PDF agrees well with this model at a longer range (beyond 3.5 Å), but a clear difference is observed between the two at a shorter range. A single, wide Mn-O peak centered at ~1.95 Å and a FWHM of 0.154 Å is observed in the crystal structure model which represents the average structure whereas two types of Mn-O bonds are clearly identified in the local structure at this temperature.

Also shown in Fig. 3 is the PDF of a model that includes local JT distortions (solid line). In this model, the apical oxygen atoms are displaced from their ideal crystallographic sites in the c direction (inset in Fig. 3). These displacements simulate a JT distortion at 50% of the Mn sites. Although the model is simple with only one unit cell, the agreement with the data is excellent particularly below 3.5 Å and represents a considerable improvement over the crystallographic model. While this model does not describe the actual directionality of the JT distortions, it provides an estimate of the concentration of the JT distorted octahedra. The orientation of the distortion can be obtained from the amplitudes of oscillation for the oxygen atoms (Table I) obtained from the thermal factors which are quite large.

The changes in the octahedral environment through the IM transition can be quantified by determining the integrated intensity of the first Mn-O peak. This peak corresponds to the number of short bonds in the octahedron alone, $N_{\text{Mn-O}}$, and its integrated intensity demonstrates how the short and long bonds vary with temperature (Fig. 4). $N_{\text{Mn-O}}$ is determined from $4\pi r^2 \rho(r)$ and normalized by the scattering lengths, with r_{min} and r_{max} as the limits of integration taken from 1.75 to 2.10 Å. The uncertainty in the upper limit can vertically shift the data points but the shape of the plot remains the same. $N_{\text{Mn-O}}$ has been determined for $LaMnO_3$ and it is exactly 4 [6]. In the crystalline model, $N_{\text{Mn-O}}$ is 6. However, in the data PDF at room temperature, $N_{\text{Mn-O}} = 5.0$ and corresponds to about 50% of the Mn sites with no long bonds (no JT effect). With cooling, the number of distorted sites decreases further corresponding to the enhancement of the charge mobility with the transition to the 3D FM ordering state. Note that $N_{\text{Mn-O}}$ does not reach 6 by 20 K which suggests that some sites are still distorted in the FM state.

An unusual increase between 200 and 300 K in $N_{\text{Mn-O}}$ is observed in Fig. 4. This coincides with the increase in the transport in the ab plane as shown in Ref. [9] where the resistivity drops along the easy axis with cooling which would invariably lead to minimization of the JT effect. The temperature at which this occurs is close to the T_C of the perovskite manganite with an equivalent amount of doping. Because of the 2D nature of the layered structure, the interlayer magnetic coupling is weaker than the intralayer coupling as the octahedra are separated by a (La/Sr-O) layer and the DE interaction between layers is weak. But the DE mechanism may occur within the bilayer in the ab plane independently of the spin ordering along the c axis. The onset of DE interactions can occur at a temperature much higher than the 3D FM ordering temperature of the layered system, closer to the ordering temperature of the perovskites. The transition in transport in the c axis occurs concomitantly to the FM ordering. But the actual decrease of the c-axis resistance is considerably smaller than the ab-plane one [9] which is consistent with the continuous change of $N_{\text{Mn-O}}$ at T_C.

The temperature dependence of the Mn-O correlations is reflected in the change of the peak height at 1.94 Å (Fig. 5). This peak corresponding to the short Mn-O bonds only exhibits the same response to temperature as

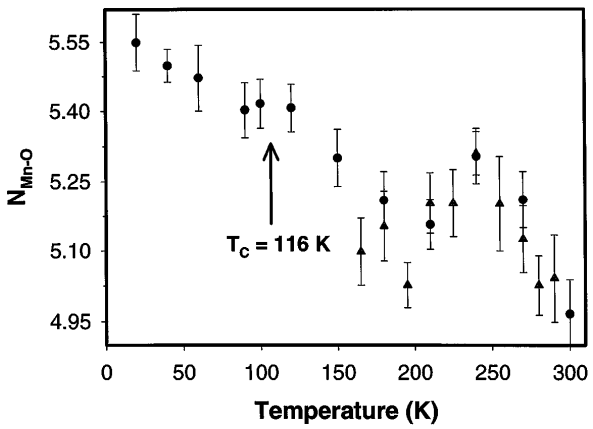

FIG. 4. The number of short Mn-O bonds, $N_{\text{Mn-O}}$, as a function of temperature. As the temperature is lowered from 300 K, $N_{\text{Mn-O}}$ increases corresponding to an increase in the number of short bonds, or a decrease in the number of Mn sites with the JT distortion. Between 200–300 K the structural changes observed are consistent with the change of the resistivity along the easy axis. Data collected at a later time (triangles) confirmed this change.

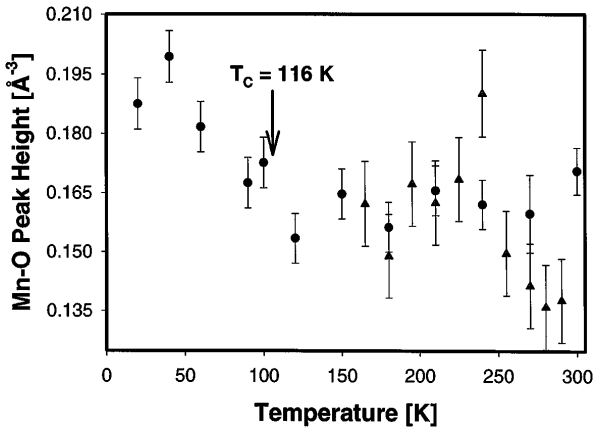

FIG. 5. The absolute PDF peak height at 1.94 Å as a function of temperature. The triangles represent data collected at a later time. This peak includes only the short Mn-O bonds of the octahedron and the increase in the height reflects the decrease in the distribution of Mn-O bonds. On cooling, the peak height exhibits a strong temperature dependence coinciding with the transition of ρ_{ab} and becomes weaker from T_C to 20 K in the 3D FM metallic phase.

the change in the concentration of $N_{\text{Mn-O}}$. From 300 K to T_C, a 27% increase in the peak height is observed while from T_C to 20 K only an 8% increase in the height occurs. Cooperative lattice changes, assisted by the magnetic ordering of the *ab* plane in the crystal, add up to increase the peak height which can also be viewed as a minimization of the distortion and reduction of the long Mn-O bonds. Thus the enhancement in the Mn-O correlations between 200–300 K reflects the increase in ρ_{ab} [9]. The smaller increase in the peak height below T_C can be correlated to the reduced effective change of the resistivity with the 3D FM transition.

In the perovskite manganites, the cooperative JT phenomena in the *ab* plane gives rise to orthorhombic splitting. In the layered manganites, even though the crystal structure is tetragonal, the octahedral bilayers are almost cubic in the average structure which may appear to suggest a very small JT distortion in this system [11,16,17]. However, this is only an average effect over the entire lattice, whereas a large JT distortion is observed *locally* in this system which is consistent with the large amplitude of oscillations for the oxygen atoms in the structure.

The JT distorted sites might be associated with regions of AFM domains observed by Perring *et al.* [10] in the PM phase. If almost half of the sites are distorted by the JT effect in the PM state, it is likely that charge hopping is allowed only in regions where no distortion is present. Thus charge hopping is in essence confined by the JT distorted sites. Within the regions of the distortion the local magnetic order can be antiferromagnetic.

In conclusion, this Letter has shown that a full local JT effect of equal magnitude to the one found in the perovskites exists in the layered manganites. A new model is proposed which takes into account a JT distortion at 50% of the Mn sites providing a better fit to the data. The structural changes observed provide a clear evidence of the lattice coupling to the 2D transport and 3D magnetic transitions in this system.

We acknowledge valuable discussions particularly with T. Egami, M. F. Hundley, and H. Röder. We thank S. Trugman, A. R. Bishop, J. L. Sarrao, and R. H. Heffner for helpful conversations and S. Short for helping with the data collection on SEPD. Work at the Los Alamos National Laboratory is performed under the auspices of the U.S. Department of Energy under Contract No. W-7405-Eng-36. The IPNS is supported by the U.S. Department of Energy, Division of Materials Sciences, under Contract No. W-31-109-Eng-38.

[1] J. Volger, Physica (Utrecht) **20**, 49 (1954); H. Jin *et al.*, Science **264**, 413 (1994); Y. Moritomo *et al.*, Phys. Rev. B **51**, 3297 (1995).
[2] C. Zener, Phys. Rev. **82**, 403 (1951); E. O. Wollan and W. C. Koehler, Phys. Rev. **100**, 545 (1955); J. B. Goodenough, Phys. Rev. **100**, 564 (1955); P. G. de Gennes, Phys. Rev. **118**, 141 (1960).
[3] Y. Tokura *et al.*, J. Phys. Soc. Jpn. B **53**, 3931 (1995).
[4] A. J. Millis, P. B. Littlewood, and B. I. Shairman, Phys. Rev. Lett. **74**, 5144 (1995); H. Röder, J. Zang, and A. R. Bishop, Phys. Rev. Lett. **76**, 1356 (1996).
[5] P. Dai *et al.*, Phys. Rev. B **54**, R3694 (1996); S. J. L. Billinge *et al.*, Phys. Rev. Lett. **77**, 715 (1996); M. F. Hundley and J. J. Neumeier, Phys. Rev. B **55**, 11 511 (1997); C. H. Booth *et al.*, Phys. Rev. B **54**, R15 606 (1996); H. Y. Hwang *et al.*, Phys. Rev. Lett. **75**, 914 (1995); T. A. Tyson *et al.*, Phys. Rev. B **53**, 13 985 (1996); W. Archibald *et al.*, Phys. Rev. B **53**, 14 445 (1996); G. Zhao *et al.*, Nature (London) **381**, 676 (1996); P. G. Radaelli *et al.*, Phys. Rev. B **54**, 8992 (1996).
[6] D. Louca and T. Egami, J. Appl. Phys. **81**, 5484 (1997); D. Louca *et al.*, Phys. Rev. B **56**, R8475 (1997).
[7] Y. Moritomo *et al.*, Nature (London) **380**, 141 (1996).
[8] S. N. Ruddlesden and P. Popper, Acta Crystallogr. **11**, 54 (1958).
[9] T. Kimura *et al.*, Science **274**, 1698 (1996).
[10] T. G. Perring *et al.*, Phys. Rev. Lett. **78**, 3197 (1997).
[11] J. F. Mitchell *et al.*, Phys. Rev. B **55**, 63 (1997).
[12] B. H. Toby and T. Egami, Acta Crystallogr. Sect. A **48**, 33 (1992); T. Egami and S. J. L. Billinge, Prog. Mater. Sci. **38**, 359 (1994). The intensity of the background has been determined by studying a standard Ni powder sample.
[13] J. F. Mitchell *et al.*, Phys. Rev. B **54**, 6172 (1996).
[14] K. R. Poeppelmeier *et al.*, J. Solid State Chem. **45**, 71 (1982).
[15] I. B. Bersuker, *Electronic Structure and Properties of Transition Metal Compounds* (John Wiley & Sons, Inc., New York, 1996), p. 297.
[16] P. D. Battle *et al.*, Chem. Mater. **9**, 1042 (1997).
[17] R. Seshadri *et al.*, Chem. Mater. **9**, 270 (1997).